

Visual adaptation stronger at horizontal than vertical meridian: Linking performance with V1 cortical surface area

Hsing-Hao Lee¹ & Marisa Carrasco^{1,2}

¹Department of Psychology, New York University, New York, NY, USA

²Center for Neural Sciences, New York University, New York, NY, USA

*Hsing-Hao Lee

Email: hsinghaolee@nyu.edu

Abstract

Visual adaptation, a mechanism that conserves bioenergetic resources by reducing energy expenditure on repetitive stimuli, leads to decreased sensitivity for similar features (e.g., orientation and spatial frequency). In human adults, visual performance declines with eccentricity and varies around polar angle for many visual dimensions and tasks: Performance is superior along the horizontal than the vertical meridian (horizontal-vertical anisotropy, HVA), and along the lower than the upper vertical meridian (vertical meridian asymmetry, VMA)(Carrasco et al., 2001). However, it remains unknown whether visual adaptation differs around polar angle. In this study, we investigated adaptation effects at the fovea and perifovea across the four cardinal locations, for horizontal and vertical adaptor and target orientations, with stimulus size adjusted as per a cortical magnification factor (Rovamo & Virsu, 1979). We measured contrast thresholds at each location separately for adaptation and non-adaptation conditions. Results confirmed the expected HVA and VMA effects in non-adapted conditions and showed they are stronger for horizontal than vertical orientations. They also revealed that, for both orientations, adaptation effects are stronger along the horizontal than the vertical meridian, which in turn is stronger than at the fovea. Furthermore, for both orientations, individual's adaptation effects at the perifoveal locations positively correlated with their cortical surface area of V1. The association of a stronger adaptation effect with larger V1 surface area suggests a more pronounced conservation of bioenergetic resources along the horizontal than the vertical meridian. Visual adaptation alleviates the HVA in contrast sensitivity, promoting a more homogeneous perception around the visual field.

Keywords: Visual adaptation; Contrast sensitivity; Polar angle asymmetries, V1 surface area

Introduction

Visual performance declines with eccentricity(1-3) and varies systematically around the polar angle: Performance is superior along the horizontal than the vertical meridian (*horizontal-vertical anisotropy*, HVA), and along the lower than the upper vertical meridian (*vertical meridian asymmetry*, VMA). Both asymmetries are pervasive across several dimensions—e.g., contrast sensitivity(4-10), spatial resolution(11-15), motion(16-20), visual acuity(21, 22)—and tasks, e.g., crowding(15, 23-26), word identification(27), and short-term memory(28).

Visual adaptation helps conserve the brain's limited bioenergetic resources by allocating less energy to repetitive stimuli(29-32). For instance, contrast adaptation reduces sensitivity(31-39) and neural responses(40-49), and recenters them away from the adaptor. Most adaptation studies have focused on the horizontal meridian (e.g.,(50-53)), and the few that tested other locations have not analyzed them separately (e.g.,(39, 54)). Thus, whether and how the adaptation effect varies around polar angle remain unknown. Moreover, the magnitude of the adaptation effect across eccentricity has yielded inconsistent findings(36, 51, 53, 54). Investigating these questions will reveal how adaptation alters perception and conserves bioenergetic resources throughout the visual field.

Here, we investigated whether adaptation decreases contrast sensitivity similarly around polar angle and at fovea. We considered three hypotheses regarding the extent of adaptation effects: (1) Uniform adaptation: Adaptation may have comparable effects around the polar angle, as early visual cortex mediates both adaptation(32, 38) and covert spatial attention^(32, 55), and attention improves performance similarly around polar angle(56-59); (2) Vertical meridian dominance: Adaptation may be stronger along the vertical (particularly at the upper) than the horizontal meridian, as adaptation depends on adaptor-target similarity(53, 54, 60), it may be stronger where population receptive fields (pRF) size is larger(61-63) and stimuli are less precisely encoded(64); (3) Horizontal meridian dominance: Adaptation may be stronger along the horizontal than the vertical meridian (particularly at the upper) given the approximately uniform density of V1 neurons across visual space(65, 66) and the larger cortical surface area devoted to the horizontal than vertical meridian and the lower than upper vertical meridian(61-63, 67-69). Locations with more neurons devoted to sensory processing elicit a stronger response to the adaptor(70, 71), and a stronger adaptor signal amplifies the adaptation effect(72-76).

Fourteen adults participated in all three experiments (**Figure 1**). In Experiment 1, participants adapted to a horizontal stimulus and discriminated whether a target Gabor, presented at the same location as the adaptor among one of four perifoveal cardinal locations, was tilted clockwise or counterclockwise from horizontal. Because sensitivity to gratings is higher in radial than tangential orientations(77-79), we anticipated an exacerbated HVA when the task involved horizontal stimulus orientation, which is radial at the horizontal meridian. To evaluate the influence of radial bias in Experiment 2 participants adapted to a vertical stimulus and discriminated whether a Gabor was tilted clockwise or counterclockwise from vertical.

In Experiment 3, we examined the adaptation effect at the fovea using the same orientation discrimination task. This addressed previous inconsistent findings and the

influence of task type on adaptation effects across eccentricity(36, 51-54, 80-82): For example, tilt aftereffects are stronger for suprathreshold targets at peripheral than central vision along the horizontal meridian(52, 53, 80-82). However, for contrast thresholds, adaptation effects are similar across foveal, parafoveal, and peripheral vision along similar along the horizontal meridian(50), and recovery times for adaptation durations ≥ 1000 ms are comparable between peripheral and foveal vision(52).

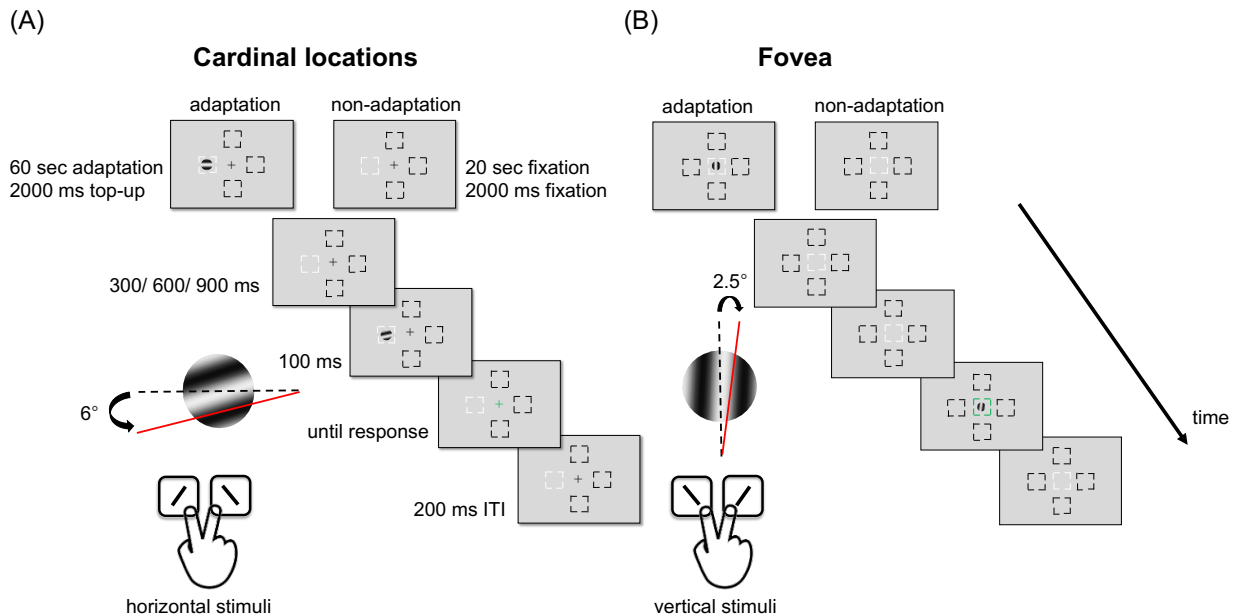


Figure 1. (A) Experimental procedure: Participants performed either adaptation or non-adaptation blocks, each in separate experimental sessions. The target Gabor stimulus was always presented within the white placeholder, and target locations were blocked. The target, a horizontal (Experiment 1) or vertical (Experiment 2) Gabor stimulus, was presented either at (A) the perifovea (Experiments 1 and 2) or (B) the fovea (Experiment 3). Participants were instructed to respond whether the Gabor was tilted clockwise or counterclockwise from horizontal (Experiment 1) or vertical (Experiment 2). The target Gabor was tilted 6° from the horizontal line or 2.5° from the vertical line. For illustration purposes, the stimulus size and spatial frequency shown here are not to scale.

Results

Experiment 1- Perifoveal Locations, Horizontal Stimulus

To investigate the adaptation effect at the vertical and horizontal meridians, we conducted a two-way ANOVA on contrast thresholds. This analysis showed a main effect of location [$F(3,39)=14.04, p<.001, \eta_p^2=0.52$] and a higher threshold in the adapted than non-adapted conditions [$F(1,13)=45.42, p<.001, \eta_p^2=0.78$], and an interaction [$F(3,39)=4.98, p=.005, \eta_p^2=0.28$], indicating that the adaptation effect varied across locations (Figure 2A).

First, we confirmed the expected HVA and VMA in the non-adaptation condition (Figure S1, upper panel). Contrast thresholds were lower along the horizontal than the vertical meridian [$t(13)=5.26, p<.001, d=1.41$] and lower at the lower than upper vertical meridian [$t(13)=3.15, p=.008, d=0.84$].

Next, we assessed the adaptation effect at the horizontal and vertical meridians. The adaptation effect (calculated as the difference between adapted and non-adapted thresholds) was stronger at the horizontal than the vertical meridian [$t(13)=3.77$, $p=.002$, $d=1.01$] (**Figures 2A, 3A**), but there was no significant difference between the upper and lower vertical meridian [$t(13)=0.01$, $p=.99$].

To account for baseline differences in the non-adapted condition, we calculated the normalized adaptation effect $[(\text{adapted threshold} - \text{non-adapted threshold}) / (\text{adapted threshold} + \text{non-adapted threshold})]$. The normalized adaptation effect was also stronger at the horizontal than the vertical meridian [$t(13)=7.84$, $p<.001$, $d=2.1$], with no significant difference at the upper and lower vertical meridians [$t(13)=1.3$, $p=.217$]. In summary, the decrease in contrast sensitivity following adaptation was more pronounced at the horizontal than the vertical meridian.

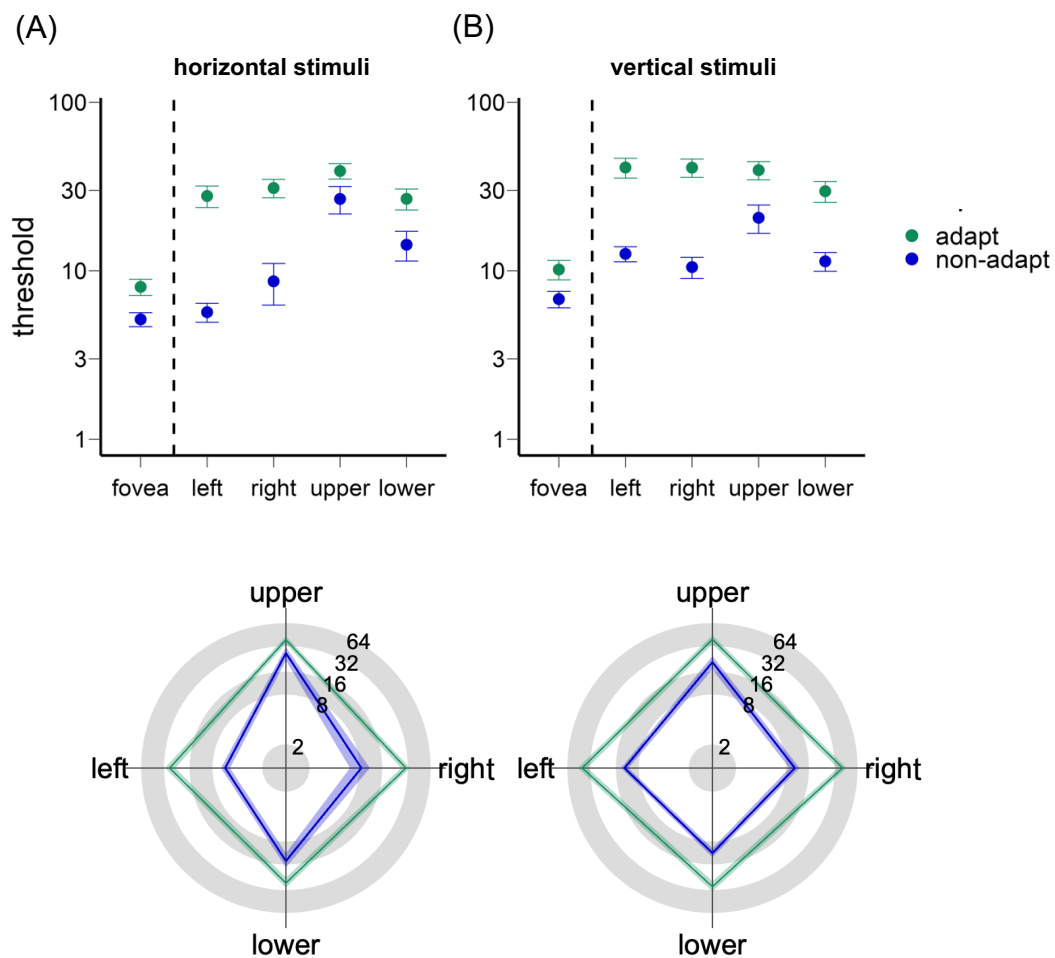


Figure 2. The contrast threshold (log-scaled) for orientation discrimination at the fovea, and at the left, right, upper, and lower perifoveal locations for **(A)** horizontal stimuli and **(B)** vertical stimuli. The adaptation effect, measured as the difference in contrast sensitivity between the adapted and non-adapted conditions, is stronger along the horizontal than the vertical meridian. The error bars represent ± 1 SEM.

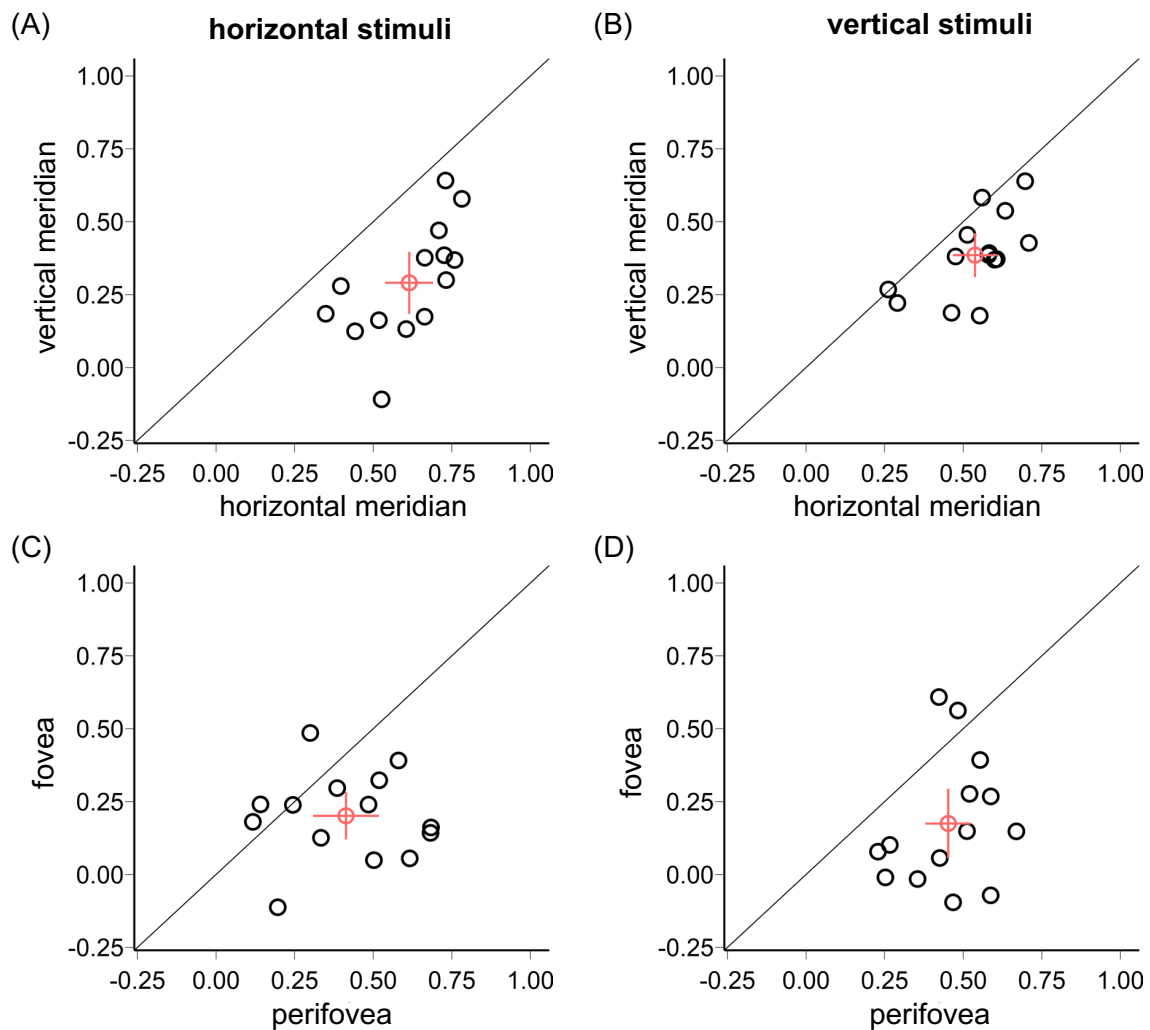


Figure 3. Upper panel: Normalized adaptation effects ((adapted – non-adapted threshold) / (adapted + non-adapted threshold)) are stronger along the horizontal than the vertical meridian for both (A) horizontal stimuli (Experiment 1) and (B) vertical stimuli (Experiment 2). Lower panel: Adaptation effects are stronger in the perifovea than the fovea for both (C) horizontal and (D) vertical stimuli. Each black circle represents the threshold ratio for an individual participant; the red circle indicates the mean across participants. Error bars represent ± 1 SEM.

Experiment 2 – Perifoveal Locations, Vertical Stimulus

When using vertical adaptor and target stimuli, the findings were consistent with those in Experiment 1. A two-way ANOVA on contrast thresholds showed main effects of location [$F(3,39)=4.59$, $p=.008$, $\eta_p^2=0.26$] and adaptation [$F(1,13)=44.15$, $p<.001$, $\eta_p^2=0.77$], as well as an interaction [$F(3,39)=6.63$, $p=.001$, $\eta_p^2=0.34$], indicating that the adaptation effect varied across locations (Figure 2B).

In the non-adapted condition (Figure S1, bottom panel), we confirmed the expected HVA and VMA. Contrast thresholds were lower along the horizontal than the vertical meridian

[$t(13)=2.18$, $p=.048$, $d=0.58$] and lower at the lower than upper vertical meridian [$t(13)=2.57$, $p=.023$, $d=0.69$].

The adaptation effect was stronger at the horizontal than the vertical meridian [$t(13)=4.04$, $p=.001$, $d=1.08$] (**Figures 2B, 3B**), but there was no significant difference between the upper and lower vertical meridian [$t(13)=0.22$, $p=.831$]. Similarly, the normalized adaptation effect was stronger at the horizontal than the vertical meridian [$t(13)=4.78$, $p<.001$, $d=1.28$], with no significant difference between the upper and lower vertical meridians [$t(13)=1.54$, $p=.147$].

Comparing adaptation between stimulus orientations

A 3-way ANOVA on contrast thresholds, with factors of location, adaptation, and stimulus orientation (horizontal: Experiment 1; vertical: Experiment 2) showed main effects of adaptation [$F(1,13)=54.22$, $p<.001$, $\eta_p^2=0.81$] and location [$F(3,39)=8.74$, $p<.001$, $\eta_p^2=0.4$], but not of stimulus orientation [$F(1,13)=1.25$, $p=.267$] or 3-way interaction [$F(3,39)<1$]. All two-way interactions emerged: location x orientation [$F(3,39)=12.33$, $p<.001$, $\eta_p^2=0.49$], adaptation x orientation [$F(1,13)=5.72$, $p=.033$, $\eta_p^2=0.31$], and adaptation x location [$F(3,39)=9.35$, $p<.001$, $\eta_p^2=0.42$].

The interaction between location and orientation (across adaptation conditions) showed a stronger HVA for horizontal than vertical stimuli [$t(13)=4.89$, $p<.001$, $d=1.31$] but no difference for the VMA [$t(13)=1.39$, $p=.187$]. The interaction between adaptation and orientation (across locations) yielded a stronger adaptation effect for the vertical than horizontal stimuli [$t(13)=2.39$, $p=.033$, $d=0.64$], but this difference was not significant for the normalized adaptation effect [$t(13)=0.78$, $p=.449$]. The interaction between adaptation and location (across orientations) reflected a stronger adaptation effect for horizontal than vertical locations, both without normalization [$t(13)=5.07$, $p<.001$, $d=1.36$], and with normalization [$t(13)=7.18$, $p<.001$, $d=1.92$].

The differences in HVA and VMA between horizontal and vertical stimuli under non-adapted conditions (**Figure S1**) resulted from a stronger HVA for horizontal stimuli [$t(13)=3.83$, $p=.002$, $d=1.03$], with no significant difference for the VMA [$t(13)=1.04$, $p=.318$, **Figure S2**].

We also found a positive correlation between normalized adaptation effects for horizontal and vertical stimuli [$r=0.46$, $p<.001$, **Figure S3A**]. This correlation remained significant after removing between-observer variability [$r=0.53$, $p<.001$, **Figure S3B**] and polar-angle differences [$r=0.3$, $p=.026$, **Figure S3C**]. These findings indicate that the adaptation effect was consistent with both stimulus orientations at the group and the individual levels.

In summary, the stronger HVA for horizontal stimuli aligns with a radial bias(77-79). The adaptation effect was stronger at the horizontal than vertical meridian, regardless of the stimulus orientation.

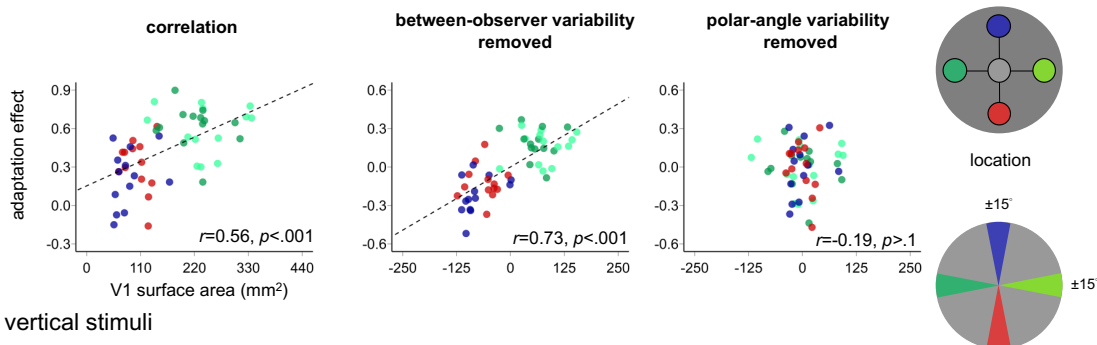
Linking brain and behavior at perifoveal locations

To test the hypothesis that cortical surface area or pRF size is related to the adaptation effect, we assessed the relation between the normalized adaptation effect and the V1

surface area for 13 out of 14 participants (one participant preferred not to be scanned). Consistent with the previous studies(61, 67, 69, 83), V1 surface area was larger along the horizontal than the vertical meridian [$t(12)=7.51, p<.001, d=2.08$], and along the lower than upper vertical meridian [$t(12)=2.37, p=.035, d=0.66$, **Figure S4**].

We observed positive correlations between the normalized adaptation effect and the V1 surface area for both horizontal [$r=0.56, p<.001$] (**Figure 4A**) and vertical [$r=0.37, p=.007$] (**Figure 4B**) stimuli (left panels). As this correlation relies on the variability across polar angles within the same observers, the data points are not independent. To evaluate the contributions of between-observer and polar-angle variability to these correlations, we regressed out these factors as described in prior research(69). First, we accounted for between-observer variability by subtracting each observer's average adaptation effect and V1 surface area values across the four polar angle locations. The positive correlations persisted for both stimulus orientations (horizontal stimulus: $r=0.73, p<.001$; vertical stimulus: $r=0.46, p<.001$; **Figure 4**, middle panels). However, when we removed variability across polar angles by subtracting the average adaptation effect and V1 surface area values for each polar angle across the 13 observers, the correlations were no longer significant (horizontal stimulus: $r=-0.003, p=.981$; vertical stimulus: $r=0.07, p=.632$; **Figure 4**, right panels). These findings indicate that the observed correlations between the adaptation effect and V1 surface area depend on the polar angle location. Indeed, averaging the V1 surface area and adaptation effect across polar angle locations eliminated the correlations (horizontal stimulus: $r=-0.19, p=.535$; vertical stimulus: $r=0.08, p=.793$).

(A) horizontal stimuli



(B) vertical stimuli

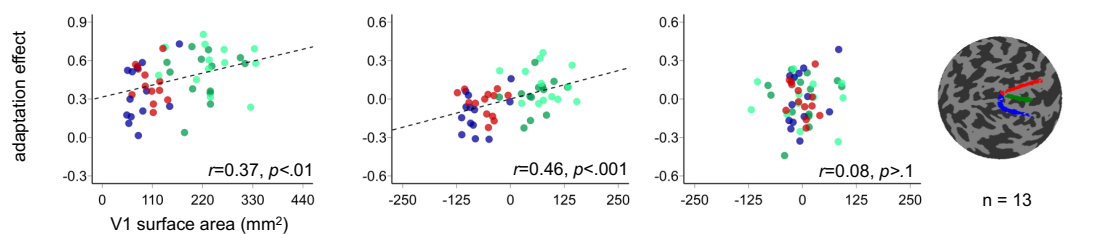


Figure 4. Correlations between the adaptation effect and V1 surface area around polar angle for (A) the horizontal stimuli and (B) vertical stimuli. Correlations are shown overall (left panels), after removing between-subject variability (middle panels), and after removing polar-angle variability (right panels). The dashed black line represents the linear fit to the data points.

Experiment 3 – Foveal Location, Horizontal and Vertical Stimuli

To compare the adaptation effect at the fovea with that at the perifovea using the same orientation discrimination task, we assessed the adaptation effect at the fovea. A two-way ANOVA on contrast thresholds yielded main effects of adaptation [$F(1,13)=17.69$, $p=.001$, $\eta_p^2=0.58$] and stimulus orientation [$F(1,13)=9.09$, $p=.01$, $\eta_p^2=0.41$] but no interaction between them [$F(1,13)<1$]. Contrast thresholds decreased after adaptation, and threshold were lower for horizontal than vertical stimuli.

We compared the normalized adaptation effect in the fovea and the perifovea. A three-way ANOVA on adaptation x location x orientation revealed an interaction: $F(1,13)=5.19$, $p=.04$, $\eta_p^2=0.29$. Thus, we conducted separate two-way location x adaptation ANOVAs for horizontal and vertical stimuli.

For the horizontal stimulus, there were main effects of location [$F(1,13)=43.93$, $p<.001$, $\eta_p^2=0.77$] and adaptation [$F(1,13)=49.25$, $p<.001$, $\eta_p^2=0.79$], as well as an interaction [$F(1,13)=33.72$, $p<.001$, $\eta_p^2=0.72$]. The adaptation effect was stronger in the perifovea than the fovea [$t(13)=5.58$, $p<.001$, $d=1.49$]. The same result emerged for the normalized adaptation effect [$t(13)=7.02$, $p<.001$, $d=1.86$] (**Figures 2A, 3C**). There was no correlation between the adaptation effect at the fovea and perifovea, either without normalization ($r=0.25$, $p=.378$) or with normalization ($r=-0.08$, $p=.777$).

For the vertical stimulus, we observed the same patterns. There were main effects of location [$F(1,13)=44.81$, $p<.001$, $\eta_p^2=0.78$] and adaptation [$F(1,13)=41.39$, $p<.001$, $\eta_p^2=0.76$], as well as an interaction [$F(1,13)=34.79$, $p<.001$, $\eta_p^2=0.73$]. Again, adaptation effects were stronger in the perifovea than fovea (**Figures 2B, 3D**) [$t(13)=6.31$, $p<.001$, $d=1.69$], and this was also the case for the normalized adaptation effect [$t(13)=5.9$, $p<.001$, $d=1.58$]. Additionally, there was no correlation between the adaptation effect at fovea and perifovea, either without normalization ($r=0.28$, $p=.332$) or with normalization ($r=0.31$, $p=.287$).

In summary, adaptation effects were consistently stronger in the perifovea than the fovea, irrespective of stimulus orientation.

Discussion

Here, we confirmed performance asymmetries in the non-adapted conditions and uncovered a stronger contrast adaptation effect at the horizontal than the vertical meridian, and in perifoveal than foveal locations, for both horizontal and vertical stimuli. The polar angle difference findings align with our third hypothesis—that locations with larger cortical surface areas have more neurons and stronger adaptor representations (70, 71), which yield a stronger adaptation effect (72-76, 84). The current study reveals that adaptation alleviated the HVA, leading to a more homogenous visibility around the visual field. Moreover, the differential adaptation effect is mediated by the larger cortical surface area at the horizontal than vertical meridian.

In the non-adapted condition, we observed the typical HVA and VMA. Both retinal and cortical factors contribute to these asymmetries. For example, retinal cone density is

higher at the horizontal than vertical meridian(85, 86), midget-RGC density is higher at the lower than upper vertical meridian(86, 87), and V1 cortical surface area is larger for the horizontal than the vertical meridian, and for the lower than upper vertical meridian (**Figure S4**;(61, 62, 67-69)). Cortical surface area accounts for more variance in behavioral asymmetries than retinal factors(88). Additionally, factors such as sensory tuning and/or neuronal computations may also contribute to these perceptual asymmetries(3, 63, 89).

This study also revealed that the HVA, but not the VMA, is stronger with horizontal than vertical stimuli. This finding is related to a radial bias(77-79); horizontal stimuli favored performance at the horizontal meridian, whereas vertical stimuli favored performance at the vertical meridian, potentiating and alleviating the HVA, respectively.

In the adaptation condition, the effect was stronger when the stimulus was vertical (2.5° target tilt) than when it was horizontal (6° target tilt). These different tilt angles were chosen to produce a comparable extent for the adaptation effect in both experiments. Our findings are consistent with previous research, which shows that the strength of adaptation decreases as the orientation difference between the target and adaptor increases(30, 35, 41, 90-94). However, once we normalized the adaptation effect as a function of the tilt angle, the difference between orientations vanished.

Adaptation reduced contrast sensitivity more along the horizontal than the vertical meridian, regardless of stimulus orientation, even after normalizing the adaptation effect.

Why was the adaptation effect stronger along the horizontal meridian? In the few contrast adaptation studies that specified the locations tested, adaptation was tested throughout the entire visual field(72, 90, 94, 95) or exclusively along the horizontal meridian(50-53). To elucidate a possible mechanism for the stronger adaptation effect at the horizontal than the vertical meridian, we consider the following points: (1) Neurostimulation studies have revealed that V1 plays a causal role in adaptation(32, 38); (2) a positive correlation exists between contrast sensitivity and V1 surface area(69); (3) there is also a positive correlation between V1 surface area and the adaptation effect (**Figure 4A, 4B**). This correlation persists after controlling for individual differences (**Figure 4B**), but not for polar angle variability (**Figure 4C**); (4) neuronal density is uniform across the visual field(65, 66). Taken together, these findings suggest that the larger surface area and higher number of neurons at the horizontal than the vertical meridian contribute to the stronger adaptation effect at the horizontal meridian.

The surface area explanation, however, does not align with the similar adaptation effects observed at the lower and upper vertical meridians. Whereas cortical surface area can account for the decline in contrast sensitivity with increasing eccentricity, it does not fully explain polar angle differences in performance(3, 96). Thus, factors beyond surface area may contribute to the observed differential adaptation effects.

Could orientation tuning play a role? The half-bandwidth of orientation selectivity is ~3-9°, but location is rarely specified in these estimates. When location is reported, this estimate is for foveal locations(92, 93) or for a wide eccentricity range(94). Future studies could address whether orientation tuning for adaptation varies across different meridians.

Likewise, were V1 surface area the sole factor underlying the extent of adaptation, the fovea would be expected to exhibit the strongest effect. However, in this study, an equated cortical size representation of the foveal stimulus(70) yielded a smaller adaptation effect in the fovea than the perifovea. These findings are consistent with some studies(53, 54), but differ from others reporting similar adaptation effects between the fovea and periphery(36, 51). Furthermore, no correlation was observed between adaptation effects in the periphery and fovea.

These results support the idea that foveal and peripheral vision are optimized for different perceptual processes(1, 2, 97). Qualitative rather than quantitative differences in processing likely mediate the observed differential adaptation effects(53). The stronger adaptation effect in the perifovea in humans is consistent with findings from macaques, where stronger contrast adaptation occurs in the retinal and geniculate cells of the peripheral magnocellular pathway than in the more foveally located parvocellular pathway(46, 98).

Like adaptation, covert attention also helps manage limited resources(29-32) and these processes interact in the early visual cortex(32). However, unlike adaptation, exogenous/involuntary(6, 7, 56, 57) or endogenous/voluntary(31, 58, 59) covert spatial(99-101) and temporal(102-104) attention enhance contrast sensitivity at the attended location. Whereas adaptation alleviates the HVA, the enhancement of spatial(6, 7, 56-59) and temporal(103) attention is similar around polar angle. Thus, covert attention neither exacerbates nor alleviates the HVA or VMA.

Presaccadic attention, which enhances contrast sensitivity at the target location right before saccade onset, also has different effects: It enhances contrast sensitivity more along the horizontal than the vertical meridian, and least at the upper vertical meridian(105-107). Consequently, presaccadic attention can exacerbate polar angle asymmetries. Interestingly, the individuals' presaccadic attention benefit negatively correlates with their V1 surface area at the upper vertical meridian, suggesting that presaccadic attention helps compensate for the reduced cortical surface area and neuronal count at that location(106). In the present study, the less pronounced adaptation effect along the vertical than the horizontal meridian may similarly reflect the smaller cortical surface area and fewer to-be-suppressed neurons by adaptation at the vertical meridian.

In conclusion, this study reveals that contrast adaptation is stronger along the horizontal than the vertical meridian, and in the periphery than the fovea, regardless of the adaptor and target orientation. Thus, contrast adaptation alleviates the HVA, contributing to a more uniform visual perception around the visual field. Moreover, consistent with the critical role of V1 plays in adaptation(32, 38), cortical V1 surface area mediates the differential adaptation effects observed between the horizontal and vertical meridians.

Materials and Methods

Participants

Fourteen adults (7 females, age range: 22-35 years old), including author HHL, participated in all three experiments. All of them had normal or corrected-to-normal vision. Sample size was based on previous studies on adaptation(32), with an effect size of $d=1.3$,

and on performance fields(105), with an effect size of $d=1.66$ for performance in the neutral trials (without attentional manipulation). According to G*Power 3.0(108), we would need 9 participants for adaptation and 7 participants for performance fields to reach a power=0.9. We also estimated the required sample size for the interaction between adaptation and location, which enable us to assess performance fields, based on a presaccadic attention and performance fields study(105), as attention and adaptation both affect contrast sensitivity(109), albeit in different directions(31, 32). Bootstrapping the observers' data from that study with 10,000 iterations showed that we would need 12 participants to reach power=0.9 for the interaction analysis. The number of participants here is similar to or higher than in previous adaptation studies (e.g.,(47, 54, 110-115)). The Institutional Review Board at New York University approved the experimental procedures, and all participants provided informed consent before they started the experiment.

Apparatus

Participants were in a dimly lit, sound-attenuated room, with their head placed on a chinrest 57 cm away from the monitor. All stimuli were generated using MATLAB (MathWorks, MA, USA) and the Psychophysics Toolbox(116, 117) on a gamma-corrected 20-inch ViewSonic G220fb CRT monitor with a spatial resolution of 1,280 x 960 pixels and a refresh rate of 100 Hz. To ensure fixation, participants' eye movements were recorded using EYELINK 1000 (SR Research, Osgoode, Ontario, Canada) with a sample rate of 1,000 Hz.

Stimuli

In Experiments 1 and 2, the target Gabor (diameter = 4° , 5 cpd, 1.25° full-width at half maximum) was presented on the left, right, upper and lower cardinal meridian locations (8° from the center to center). There were four placeholders (length = 0.16° , width = 0.06°) 0.5° away from Gabor's edge. The fixation cross consisted of a plus sign (length = 0.25° ; width = 0.06°) at the center of the screen.

In Experiment 3, the fixation was replaced by a white placeholder, which was the same size as the other placeholders. We adjusted the target Gabor size according to the Cortical Magnification Factor(70) averaged from nasal, temporal, superior, and inferior formulas(3, 118, 119), which yielded a 1.03° diameter and presented it at the center (0° eccentricity).

Experimental design and procedures

Figure 1 shows the procedure of the task. In the adaptation condition, at the beginning of each block, participants adapted to a horizontal Gabor patch (5 cpd) flickering at 7.5 Hz in a counterphase manner presented at the target location for 60 seconds. Each trial started with 2s top-up phase to ensure a continuous adaptation effect throughout the block. In the non-adaptation condition, participants maintained fixation at the center for 20s (without Gabor) at the beginning of each block and for 2s at the beginning of each trial.

After the top-up, there was a 300, 600 or 900 ms jitter before a tilted Gabor was presented for 100 ms. The fixation plus-sign turned green as a response cue. Participants had to judge whether the target was tilted clockwise or counterclockwise off horizontal or vertical in Experiments 1 and 2, respectively. In Experiment 3, they responded off horizontal or vertical in different experimental sessions. The tilt angle was 6° away from the horizontal

line and 2.5° away from the vertical line. They were based on pilot data to ensure an adaptation effect while avoiding floor or ceiling performance.

A feedback tone was presented when participants gave an incorrect response. The target locations were blocked. Participants were asked to respond as accurately as possible while fixating at the center of the screen throughout the trial. A trial would be aborted and repeated at the end of the block if participants' eyes position deviated $\geq 1.25^\circ$ from the center from the onset of the adaptation top-up until the response cue onset. There were 48 trials in each block, 4 blocks (192 trials per location for each adaptation and non-adaptation conditions) were conducted consecutively at each location.

In Experiment 1, participants completed the adaptation and non-adaptation conditions on different days, with a counterbalanced order. In Experiments 2 and 3, participants conducted the non-adapted condition followed by the adapted condition. In both Experiments 1 and 2, the order of the target locations was counterbalanced across participants. In Experiment 3, the two stimulus orientation conditions were conducted on different days (one observer the same day but an hour apart) to eliminate any carry-over effect. All observers participated in a practice session to familiarize themselves with the task procedure.

Titration procedures

We titrated the contrast threshold of the Gabor separately for each location (central, left, right, upper, lower) and adaptation condition (adaptation, non-adaptation) with an adaptive staircase procedure using the Palamedes toolbox(120), as in previous studies(32, 55, 105, 121). There were 4 independent staircases for each condition, varying Gabor contrast from 2% to 85% to reach $\sim 75\%$ accuracy for the orientation discrimination task. Each staircase started from 4 different points (85%, 2%, 43.5% the median, and a random point between 2% and 85%) and contained 48 trials. We averaged the last 8 trials to derive the contrast threshold. The few outlier staircases (3.3%), defined as the threshold $0.5 \log_{10}$ away from the mean of other staircases in that condition(105), were excluded from data analysis.

Psychometric function fitting

We fitted a Weibull function for the accuracy as a function of contrast threshold. For each condition, a logistic function was fit to the data using maximum likelihood estimation using the `fmincon` function in MATLAB. The results derived from the psychometric function estimation positively correlated ($p < .01$) with the staircase results in all experiments, verifying our procedure in all conditions.

Behavioral data analyses

Behavioral data analyses were performed using R(122). In Experiments 1 and 2, a two-way repeated-measures analysis of variance (ANOVA) on contrast threshold was conducted on the factors of location (left, right, upper, lower) and adaptation (adapted, non-adapted) conditions to assess statistical significance. We also compared the thresholds in a 3-way repeated-measures ANOVA on the factors of location (left, right, upper, lower), adaptation (adapted, non-adapted), and stimulus orientation (vertical, horizontal) across Experiments 1 and 2. In Experiment 3, we compared the contrast

threshold in the fovea and periphery by pooling the performance across all locations in the periphery.

Repeated-measures ANOVA along with effect size (η^2) were computed in R(122) and used to assess statistical significance. η_p^2 was provided for all F tests, where $\eta_p^2=0.01$ indicates small effect, $\eta_p^2=0.06$ indicates a medium effect, and $\eta_p^2=0.14$ indicates a large effect. *Cohen's d* was also computed for each post-hoc t -test, where $d=0.2$ indicates a small effect, $d=0.5$ indicates a medium effect, and $d=0.8$ indicates a large effect(123).

The adaptation effect was quantified as the difference between the adapted and non-adapted threshold. We also quantified the normalized adaptation effect based on [(adapted threshold–non-adapted threshold)/(adapted threshold+non-adapted threshold)], similar to quantification of attentional effects (e.g.,(75, 124, 125)), which takes into account the baseline difference in the non-adapted condition.

The pRF analysis and correlation with the adaptation effect

We were able to obtain population receptive fields (pRF;(126)) and anatomical data for 13 out of 14 observers from the NYU Retinotopy Database(68). One participant preferred not to be scanned. The pRF stimulus, MRI, and fMRI acquisition parameters and preprocessing, the implementation of the pRF model, and the calculation of V1 surface area were identical to those described in the previous work(3, 68, 106). In brief, we computed the amount of V1 surface area representing the left HM, right HM, upper VM, and lower VM by defining $\pm 15^\circ$ wedge-ROIs in the visual field (centered along the 4 cardinal locations) using the distance maps, as in previous studies (e.g.,(62, 69)). The cortical distance maps specify the distance of each vertex from the respective cardinal meridian (in mm), with the distance of the meridian itself set to 0 mm. Each ROI extended from 4° to 12° eccentricity. We did not analyze the cortical surface corresponding to the fovea because noise in the pRF estimates of retinotopic coordinates near the foveal confluence tends to be large(62, 68, 127, 128), and the fixation task covered the central 0.5° of the display during the pRF mapping measurement. The amount of V1 surface area (in mm^2) was calculated using the average distance of a pool of vertices whose pRF polar angle coordinates lie near the edge of the 15° boundary in visual space, and we excluded vertices outside 30° away from the wedge-ROI center to preclude the noise. Two researchers (including the first author HHL) independently drew the distance maps for the dorsal and ventral part of V1 by hand using neuropathy (<https://github.com/noahbenson/neuropathy>;(129)). The horizontal distance map was derived by the average of the dorsal and ventral maps. These steps were completed for left and right hemisphere of V1 respectively. We then summed through the vertices that had distance within the mean distance calculated for reach cardinal location. Total V1 surface area was highly consistent between independent delineations by two researchers ($r=0.99$, $p<.001$). We then averaged the calculated V1 surface area between the ROIs drawn by the two researchers, as in a previous study(130), and then conducted correlation analysis to evaluate the relation between V1 surface area and the adaptation effect at the individual level.

Acknowledgments

This research was supported by NIH NEI R01-EY027401 to M.C. and the Ministry of Education in Taiwan to H.H.L. We thank Rania Ezzo for her assistance in data acquisition

for the MRI data, and Marc Himmelberg, Jan Kurzawski, and David Tu for their help in analyzing the pRF data. We also thank Carrasco Lab members, especially Marc Himmelberg, Ekin Tünçok and Shutian Xue, for their helpful comments on the manuscript.

References

1. H. Strasburger, I. Rentschler, M. Jüttner, Peripheral vision and pattern recognition: A review. *Journal of Vision* **11**, 13 (2011).
2. K. Anton-Erxleben, M. Carrasco, Attentional enhancement of spatial resolution: Linking behavioural and neurophysiological evidence. *Nature Reviews Neuroscience* **14**, 188-200 (2013).
3. M. Jigo, D. Tavdy, M. M. Himmelberg, M. Carrasco, Cortical magnification eliminates differences in contrast sensitivity across but not around the visual field. *elife* **12**, e84205 (2023).
4. J. Abrams, A. Nizam, M. Carrasco, Isoeccentric locations are not equivalent: The extent of the vertical meridian asymmetry. *Vision Research* **52**, 70-78 (2012).
5. A. S. Baldwin, T. S. Meese, D. H. Baker, The attenuation surface for contrast sensitivity has the form of a witch's hat within the central visual field. *Journal of Vision* **12**, 23 (2012).
6. E. L. Cameron, J. C. Tai, M. Carrasco, Covert attention affects the psychometric function of contrast sensitivity. *Vision Research* **42**, 949-967 (2002).
7. M. Carrasco, C. P. Talgar, E. L. Cameron, Characterizing visual performance fields: Effects of transient covert attention, spatial frequency, eccentricity, task and set size. *Spatial Vision* **15**, 61 (2001).
8. J. E. Corbett, M. Carrasco, Visual performance fields: Frames of reference. *PLoS One* **6**, e24470 (2011).
9. S. Fuller, R. Z. Rodriguez, M. Carrasco, Apparent contrast differs across the vertical meridian: Visual and attentional factors. *Journal of Vision* **8**, 16 (2008).
10. M. M. Himmelberg, J. Winawer, M. Carrasco, Stimulus-dependent contrast sensitivity asymmetries around the visual field. *Journal of Vision* **20**, 18 (2020).
11. T. A. Nazir, Effects of lateral masking and spatial precueing on gap-resolution in central and peripheral vision. *Vision Research* **32**, 771-777 (1992).
12. E. Altpeter, M. Mackeben, S. Trauzettel-Klosinski, The importance of sustained attention for patients with maculopathies. *Vision Research* **40**, 1539-1547 (2000).
13. M. Carrasco, P. E. Williams, Y. Yeshurun, Covert attention increases spatial resolution with or without masks: Support for signal enhancement. *Journal of Vision* **2**, 4 (2002).
14. C. P. Talgar, M. Carrasco, Vertical meridian asymmetry in spatial resolution: Visual and attentional factors. *Psychonomic Bulletin & Review* **9**, 714-722 (2002).
15. J. A. Greenwood, M. Szinte, B. Sayim, P. Cavanagh, Variations in crowding, saccadic precision, and spatial localization reveal the shared topology of spatial vision. *Proceedings of the National Academy of Sciences* **114**, E3573-E3582 (2017).
16. T. Naito, Y. Kaneoke, N. Osaka, R. Kakigi, Asymmetry of the human visual field in magnetic response to apparent motion. *Brain Research* **865**, 221-226 (2000).
17. L. Lakha, G. Humphreys, Lower visual field advantage for motion segmentation during high competition for selection. *Spatial Vision* **18** (2005).
18. S. Fuller, M. Carrasco, Perceptual consequences of visual performance fields: The case of the line motion illusion. *Journal of Vision* **9**, 13 (2009).

19. K. S. Pilz, D. Papadaki, An advantage for horizontal motion direction discrimination. *Vision Research* **158**, 164-172 (2019).
20. E. Tünçok, L. Kiorpes, M. Carrasco, Opposite asymmetry in visual perception of humans and macaques. *Current Biology* (2024).
21. A. Barbot, S. Xue, M. Carrasco, Asymmetries in visual acuity around the visual field. *Journal of Vision* **21**, 2 (2021).
22. Y. Kwak, N. M. Hanning, M. Carrasco, Presaccadic attention sharpens visual acuity. *Scientific Reports* **13**, 2981 (2023).
23. Y. Petrov, O. Meleshkevich, Asymmetries and idiosyncratic hot spots in crowding. *Vision Research* **51**, 1117-1123 (2011).
24. T. S. Wallis, P. J. Bex, Image correlates of crowding in natural scenes. *Journal of Vision* **12**, 6 (2012).
25. F. C. Fortenbaugh, M. A. Silver, L. C. Robertson, Individual differences in visual field shape modulate the effects of attention on the lower visual field advantage in crowding. *Journal of Vision* **15**, 19 (2015).
26. J. W. Kurzawski *et al.*, The Bouma law accounts for crowding in 50 observers. *Journal of Vision* **23**, 6 (2023).
27. L.-T. Tsai, K.-M. Liao, C.-H. Hou, Y. Jang, C.-C. Chen, Visual field asymmetries in visual word form identification. *Vision Research* **220**, 108413 (2024).
28. L. Montaser-Kouhsari, M. Carrasco, Perceptual asymmetries are preserved in short-term memory tasks. *Attention, Perception, & Psychophysics* **71**, 1782-1792 (2009).
29. P. Lennie, The cost of cortical computation. *Current Biology* **13**, 493-497 (2003).
30. A. Kohn, Visual adaptation: Physiology, mechanisms, and functional benefits. *Journal of Neurophysiology* **97**, 3155-3164 (2007).
31. F. Pestilli, G. Viera, M. Carrasco, How do attention and adaptation affect contrast sensitivity? *Journal of Vision* **7**, 9 (2007).
32. H.-H. Lee, A. Fernández, M. Carrasco, Adaptation and exogenous attention interact in the early visual cortex: A TMS study. *iScience* 10.1016/j.isci.2024.111155 (2024).
33. R. Dealy, D. Tolhurst, Is spatial adaptation an after-effect of prolonged inhibition? *The Journal of Physiology* **241**, 261-270 (1974).
34. D. Rose, An investigation into hemisphere differences in adaptation to contrast. *Perception & Psychophysics* **34**, 89-95 (1983).
35. A. Bradley, E. Switkes, K. De Valois, Orientation and spatial frequency selectivity of adaptation to color and luminance gratings. *Vision Research* **28**, 841-856 (1988).
36. S. Anstis, Adaptation to peripheral flicker. *Vision Research* **36**, 3479-3485 (1996).
37. D. Y. Dao, Z.-L. Lu, B. A. Doshier, Adaptation to sine-wave gratings selectively reduces the contrast gain of the adapted stimuli. *Journal of Vision* **6**, 6 (2006).
38. F. Perini, L. Cattaneo, M. Carrasco, J. V. Schwarzbach, Occipital transcranial magnetic stimulation has an activity-dependent suppressive effect. *Journal of Neuroscience* **32**, 12361-12365 (2012).
39. M. Bao, E. Fast, J. Mesik, S. Engel, Distinct mechanisms control contrast adaptation over different timescales. *Journal of Vision* **13**, 14 (2013).
40. L. Maffei, A. Fiorentini, S. Bisti, Neural correlate of perceptual adaptation to gratings. *Science* **182**, 1036-1038 (1973).

41. M. W. Greenlee, S. Magnussen, Interactions among spatial frequency and orientation channels adapted concurrently. *Vision Research* **28**, 1303-1310 (1988).
42. G. Sclar, P. Lennie, D. D. DePriest, Contrast adaptation in striate cortex of macaque. *Vision Research* **29**, 747-755 (1989).
43. M. Carandini, D. Ferster, A tonic hyperpolarization underlying contrast adaptation in cat visual cortex. *Science* **276**, 949-952 (1997).
44. M. Carandini, J. A. Movshon, D. Ferster, Pattern adaptation and cross-orientation interactions in the primary visual cortex. *Neuropharmacology* **37**, 501-511 (1998).
45. G. M. Boynton, E. M. Finney, Orientation-specific adaptation in human visual cortex. *Journal of Neuroscience* **23**, 8781-8787 (2003).
46. S. G. Solomon, J. W. Peirce, N. T. Dhruv, P. Lennie, Profound contrast adaptation early in the visual pathway. *Neuron* **42**, 155-162 (2004).
47. F. Fang, S. He, Viewer-centered object representation in the human visual system revealed by viewpoint aftereffects. *Neuron* **45**, 793-800 (2005).
48. T. Duong, R. D. Freeman, Spatial frequency-specific contrast adaptation originates in the primary visual cortex. *Journal of Neurophysiology* **98**, 187-195 (2007).
49. M. Vergeer, J. Mesik, Y. Baek, K. Wilmerding, S. A. Engel, Orientation-selective contrast adaptation measured with SSVEP. *Journal of Vision* **18**, 2 (2018).
50. A. Beaton, C. Blakemore, Orientation selectivity of the human visual system as a function of retinal eccentricity and visual hemifield. *Perception* **10**, 273-282 (1981).
51. S. Schieting, L. Spillmann, Flicker adaptation in the peripheral retina. *Vision Research* **27**, 277-284 (1987).
52. M. W. Greenlee, M. A. Georgeson, S. Magnussen, J. P. Harris, The time course of adaptation to spatial contrast. *Vision Research* **31**, 223-236 (1991).
53. Y. Gao, M. A. Webster, F. Jiang, Dynamics of contrast adaptation in central and peripheral vision. *Journal of Vision* **19**, 23 (2019).
54. E. Gheorghiu, J. Bell, R. Gurnsey, Why do shape aftereffects increase with eccentricity? *Journal of Vision* **11**, 18 (2011).
55. A. Fernández, M. Carrasco, Extinguishing exogenous attention via transcranial magnetic stimulation. *Current Biology* **30**, 4078-4084. e4073 (2020).
56. M. Roberts, R. Cymerman, R. T. Smith, L. Kiorpes, M. Carrasco, Covert spatial attention is functionally intact in amblyopic human adults. *Journal of Vision* **16**, 30 (2016).
57. M. Roberts, B. Ashinoff, F. Castellanos, M. Carrasco, Endogenous and exogenous covert attention are functionally intact in adults with ADHD. *Journal of Vision* **17**, 699 (2017).
58. S. Purokayastha, M. Roberts, M. Carrasco, Voluntary attention improves performance similarly around the visual field. *Attention, Perception, & Psychophysics* **83**, 2784-2794 (2021).
59. E. Tünçok, M. Carrasco, J. Winawer, Spatial attention alters visual cortical representation during target anticipation. *bioRxiv*, 2024.2003. 2002.583127 (2024).
60. E. Gheorghiu, J. Bell, F. A. Kingdom, Line orientation adaptation: Local or global? *PLoS One* **8**, e73307 (2013).
61. M. F. Silva *et al.*, Radial asymmetries in population receptive field size and cortical magnification factor in early visual cortex. *NeuroImage* **167**, 41-52 (2018).

62. M. M. Himmelberg *et al.*, Comparing retinotopic maps of children and adults reveals a late-stage change in how V1 samples the visual field. *Nature Communications* **14**, 1561 (2023).
63. M. M. Himmelberg, J. Winawer, M. Carrasco, Polar angle asymmetries in visual perception and neural architecture. *Trends in Neurosciences* **46**, 445-458 (2023).
64. J. Winawer, H. Horiguchi, Population receptive field size estimates in 3 human retinotopic maps. (2015).
65. D. H. Hubel, T. N. Wiesel, Ferrier lecture-Functional architecture of macaque monkey visual cortex. *Proceedings of the Royal Society of London. Series B. Biological Sciences* **198**, 1-59 (1977).
66. A. Rockel, R. W. Hiorns, T. Powell, The basic uniformity in structure of the neocortex. *Brain* **103**, 221-244 (1980).
67. N. C. Benson, E. R. Kupers, A. Barbot, M. Carrasco, J. Winawer, Cortical magnification in human visual cortex parallels task performance around the visual field. *elife* **10**, e67685 (2021).
68. M. M. Himmelberg *et al.*, Cross-dataset reproducibility of human retinotopic maps. *Neuroimage* **244**, 118609 (2021).
69. M. M. Himmelberg, J. Winawer, M. Carrasco, Linking individual differences in human primary visual cortex to contrast sensitivity around the visual field. *Nature Communications* **13**, 3309 (2022).
70. J. Rovamo, V. Virsu, An estimation and application of the human cortical magnification factor. *Experimental Brain Research* **37**, 495-510 (1979).
71. A. Peters, "Number of neurons and synapses in primary visual cortex" in *Cerebral cortex: Further aspects of cortical function, including hippocampus*. (Springer, 1987), pp. 267-294.
72. J. L. Gardner *et al.*, Contrast adaptation and representation in human early visual cortex. *Neuron* **47**, 607-620 (2005).
73. R. Blake, D. Tadin, K. V. Sobel, T. A. Raissian, S. C. Chong, Strength of early visual adaptation depends on visual awareness. *Proceedings of the National Academy of Sciences* **103**, 4783-4788 (2006).
74. N. A. Crowder *et al.*, Relationship between contrast adaptation and orientation tuning in V1 and V2 of cat visual cortex. *Journal of Neurophysiology* **95**, 271-283 (2006).
75. T. Liu, J. Larsson, M. Carrasco, Feature-based attention modulates orientation-selective responses in human visual cortex. *Neuron* **55**, 313-323 (2007).
76. J. Larsson, A. T. Smith, fMRI repetition suppression: Neuronal adaptation or stimulus expectation? *Cerebral Cortex* **22**, 567-576 (2012).
77. Y. Sasaki *et al.*, The radial bias: A different slant on visual orientation sensitivity in human and nonhuman primates. *Neuron* **51**, 661-670 (2006).
78. R. Ezzo, J. Winawer, M. Carrasco, B. Rokers, Asymmetries in the discrimination of motion direction around the visual field. *Journal of Vision* **23**, 19 (2023).
79. J. Ryu, S.-H. Lee, Bounded contribution of human early visual cortex to the topographic anisotropy in spatial extent perception. *Communications Biology* **7**, 178 (2024).
80. D. Muir, R. Over, Tilt aftereffects in central and peripheral vision. *Journal of Experimental Psychology* **85**, 165 (1970).
81. R. Over, J. Broerse, B. Crassini, Orientation illusion and masking in central and peripheral vision. *Journal of Experimental Psychology* **96**, 25 (1972).

82. J. Harris, J. Calvert, Contrast, spatial frequency and test duration effects on the tilt aftereffect: Implications for underlying mechanisms. *Vision Research* **29**, 129-135 (1989).
83. C. O'Connell *et al.*, Structural and functional correlates of visual field asymmetry in the human brain by diffusion kurtosis MRI and functional MRI. *Neuroreport* **27**, 1225-1231 (2016).
84. E. Tring, M. Dipoppa, D. L. Ringach, On the contrast response function of adapted neural populations. *Journal of Neurophysiology* **131**, 446-453 (2024).
85. C. A. Curcio, K. R. Sloan Jr, O. Packer, A. E. Hendrickson, R. E. Kalina, Distribution of cones in human and monkey retina: individual variability and radial asymmetry. *Science* **236**, 579-582 (1987).
86. C. A. Curcio, K. R. Sloan, R. E. Kalina, A. E. Hendrickson, Human photoreceptor topography. *Journal of Comparative Neurology* **292**, 497-523 (1990).
87. H. Song, T. Y. P. Chui, Z. Zhong, A. E. Elsner, S. A. Burns, Variation of cone photoreceptor packing density with retinal eccentricity and age. *Investigative Ophthalmology & Visual Science* **52**, 7376-7384 (2011).
88. E. R. Kupers, N. C. Benson, M. Carrasco, J. Winawer, Asymmetries around the visual field: From retina to cortex to behavior. *PLoS Computational Biology* **18**, e1009771 (2022).
89. S. Xue, M. Carrasco, Featural representation underlies performance differences around the visual field. *Journal of Vision* **23**, 4771 (2023).
90. F. Fang, S. O. Murray, D. Kersten, S. He, Orientation-tuned fMRI adaptation in human visual cortex. *Journal of Neurophysiology* **94**, 4188-4195 (2005).
91. C. Blakemore, J. Nachmias, The orientation specificity of two visual after-effects. *The Journal of Physiology* **213**, 157-174 (1971).
92. R. J. Snowden, Measurement of visual channels by contrast adaptation. *Proceedings of the Royal Society of London. Series B: Biological Sciences* **246**, 53-59 (1991).
93. G. C. Phillips, H. R. Wilson, Orientation bandwidths of spatial mechanisms measured by masking. *JOSA A* **1**, 226-232 (1984).
94. J. Larsson, S. J. Harrison, Spatial specificity and inheritance of adaptation in human visual cortex. *Journal of Neurophysiology* **114**, 1211-1226 (2015).
95. L. N. Vinke, I. M. Bloem, S. Ling, Saturating nonlinearities of contrast response in human visual cortex. *Journal of Neuroscience* **42**, 1292-1302 (2022).
96. S. Xue, A. Fernández, M. Carrasco, Featural representation and internal noise underlie the eccentricity effect in contrast sensitivity. *Journal of Neuroscience* **44** (2024).
97. R. Rosenholtz, Capabilities and limitations of peripheral vision. *Annual Review of Vision Science* **2**, 437-457 (2016).
98. A. J. Camp, C. Tailby, S. G. Solomon, Adaptable mechanisms that regulate the contrast response of neurons in the primate lateral geniculate nucleus. *Journal of Neuroscience* **29**, 5009-5021 (2009).
99. S. Ling, M. Carrasco, Sustained and transient covert attention enhance the signal via different contrast response functions. *Vision Research* **46**, 1210-1220 (2006).
100. F. Pestilli, M. Carrasco, Attention enhances contrast sensitivity at cued and impairs it at uncued locations. *Vision Research* **45**, 1867-1875 (2005).
101. F. Pestilli, S. Ling, M. Carrasco, A population-coding model of attention's influence on contrast response: Estimating neural effects from psychophysical data. *Vision Research* **49**, 1144-1153 (2009).

102. R. N. Denison, D. J. Heeger, M. Carrasco, Attention flexibly trades off across points in time. *Psychonomic Bulletin & Review* **24**, 1142-1151 (2017).
103. A. Fernández, R. N. Denison, M. Carrasco, Temporal attention improves perception similarly at foveal and parafoveal locations. *Journal of Vision* **19**, 12 (2019).
104. R. N. Denison, Visual temporal attention from perception to computation. *Nature Reviews Psychology* **3**, 261-274 (2024).
105. N. M. Hanning, M. M. Himmelberg, M. Carrasco, Presaccadic attention enhances contrast sensitivity, but not at the upper vertical meridian. *Isience* **25** (2022).
106. N. M. Hanning, M. M. Himmelberg, M. Carrasco, Presaccadic attention depends on eye movement direction and is related to V1 cortical magnification. *Journal of Neuroscience* **44** (2024).
107. Y. Kwak, Y. Zhao, Z.-L. Lu, N. M. Hanning, M. Carrasco, Presaccadic attention enhances and reshapes the Contrast Sensitivity Function differentially around the visual field. *eNeuro* **11** (2024).
108. F. Faul, E. Erdfelder, A.-G. Lang, A. Buchner, G* Power 3: A flexible statistical power analysis program for the social, behavioral, and biomedical sciences. *Behavior Research Methods* **39**, 175-191 (2007).
109. M. Carrasco, Visual attention: The past 25 years. *Vision Research* **51**, 1484-1525 (2011).
110. S.-L. Yeh, I. Chen, K. K. De Valois, R. L. De Valois, Figural aftereffects and spatial attention. *Journal of Experimental Psychology: Human Perception and Performance* **22**, 446 (1996).
111. D. Melcher, Spatiotopic transfer of visual-form adaptation across saccadic eye movements. *Current Biology* **15**, 1745-1748 (2005).
112. A. Ezzati, A. Golzar, A. S. Afraz, Topography of the motion aftereffect with and without eye movements. *Journal of Vision* **8**, 23 (2008).
113. K. Anton-Erxleben, K. Herrmann, M. Carrasco, Independent effects of adaptation and attention on perceived speed. *Psychological Science* **24**, 150-159 (2013).
114. A. Barbot, M. Carrasco, Attention modifies spatial resolution according to task demands. *Psychological Science* **28**, 285-296 (2017).
115. S. L. Fairhall, J. Schwarzbach, A. Lingnau, M. G. Van Koningsbruggen, D. Melcher, Spatiotopic updating across saccades revealed by spatially-specific fMRI adaptation. *Neuroimage* **147**, 339-345 (2017).
116. D. H. Brainard, The psychophysics toolbox. *Spatial Vision* **10**, 433-436 (1997).
117. D. G. Pelli, The VideoToolbox software for visual psychophysics: Transforming numbers into movies. *Spatial Vision* **10**, 437-442 (1997).
118. M. Carrasco, T. L. McLean, S. M. Katz, K. S. Frieder, Feature asymmetries in visual search: Effects of display duration, target eccentricity, orientation and spatial frequency. *Vision Research* **38**, 347-374 (1998).
119. S. J. Prince, B. J. Rogers, Sensitivity to disparity corrugations in peripheral vision. *Vision Research* **38**, 2533-2537 (1998).
120. N. Prins, F. A. Kingdom, Applying the model-comparison approach to test specific research hypotheses in psychophysical research using the Palamedes toolbox. *Frontiers in Psychology* **9**, 1250 (2018).
121. M. Jigo, M. Carrasco, Attention alters spatial resolution by modulating second-order processing. *Journal of Vision* **18**, 2 (2018).
122. R. C. Team, R language definition. *Vienna, Austria: R foundation for statistical computing* **3**, 116 (2000).

123. J. Cohen, *Statistical power analysis for the behavioral sciences* (Routledge, 2013).
124. E. A. Buffalo, P. Fries, R. Landman, H. Liang, R. Desimone, A backward progression of attentional effects in the ventral stream. *Proceedings of the National Academy of Sciences* **107**, 361-365 (2010).
125. A. M. Ni, J. H. Maunsell, Spatially tuned normalization explains attention modulation variance within neurons. *Journal of Neurophysiology* **118**, 1903-1913 (2017).
126. S. O. Dumoulin, B. A. Wandell, Population receptive field estimates in human visual cortex. *Neuroimage* **39**, 647-660 (2008).
127. R. F. Dougherty *et al.*, Visual field representations and locations of visual areas V1/2/3 in human visual cortex. *Journal of Vision* **3**, 1 (2003).
128. M. M. Schira, C. W. Tyler, M. Breakspear, B. Spehar, The foveal confluence in human visual cortex. *Journal of Neuroscience* **29**, 9050-9058 (2009).
129. N. C. Benson, J. Winawer, Bayesian analysis of retinotopic maps. *elife* **7**, e40224 (2018).
130. J. W. Kurzawski *et al.*, Human V4 size predicts crowding distance. *bioRxiv*, 2024.2004.2003.587977 (2024).